Hindawi
International Journal of Differential Equations
Volume 2023, Article ID 1240970, 19 pages
https://doi.org/10.1155/2023/1240970

Research Article

Solving Nonlinear Fractional PDEs with Applications to Physics and Engineering Using the Laplace Residual Power Series Method

Khalid K. Ali,[1] **F. E. Abd Elbary**,[2] **Mohamed S. Abdel-Wahed**,[3] **M. A. Elsisy**,[3] **and Mourad S. Semary**[3]

[1]*Mathematics Department, Faculty of Science, Al-Azhar University, Nasr-City, Cairo, Egypt*
[2]*Faculty of Engineering, MTI University, Cairo, Egypt*
[3]*Department of Basic Engineering Sciences, Faculty of Engineering at Benha, Benha University, Cairo, Egypt*

Correspondence should be addressed to Khalid K. Ali; khalidkaram2012@azhar.edu.eg

Received 29 September 2023; Revised 8 November 2023; Accepted 8 December 2023; Published 27 December 2023

Academic Editor: Igor Freire

The Laplace residual power series (LRPS) method uses the Caputo fractional derivative definition to solve nonlinear fractional partial differential equations. This technique has been applied successfully to solve equations such as the fractional Kuramoto–Sivashinsky equation (FKSE) and the fractional generalized regularized long wave equation (GRLWE). By transforming the equation into the Laplace domain and replacing fractional derivatives with integer derivatives, the LRPS method can solve the resulting equation using a power series expansion. The resulting solution is accurate and convergent, as demonstrated in this paper by comparing it with other analytical methods. The LRPS approach offers both computational efficiency and solution accuracy, making it an effective technique for solving nonlinear fractional partial differential equations (NFPDEs). The results are presented in the form of graphs for various values of the order of the fractional derivative and time, and the essential objective is to reduce computation effort.

1. Introduction

In recent years, fractional calculus has gained significant attention from scientists and engineers due to its broad applicability and its ability to capture the complexities of real-world problems in various fields such as plasma physics, fluid dynamics, quantum mechanics, optics, and signal processing. Its use has allowed for a more accurate representation of these phenomena and has provided insights that traditional calculus cannot capture [1, 2]. Fractional partial differential equations (FPDEs) are widely used in various scientific and technological fields, and many researchers have been studying them lately. These fractional equations can describe many interesting phenomena in the areas of fluid and quantum mechanics, waves and optical fiber, electrodynamics, material science, plasma physics, and more [3, 4].

Numerous techniques have been suggested in previous studies to solve these equations. Some of these are FADM [5], RDTM [6], ILTM [7], ETDM [8], and more [9, 10]. Our goal in this paper is to use LRPSM to solve the following two equations.

1.1. Fractional Generalized Kuramoto–Sivashinsky Equation. The fractional generalized Kuramoto–Sivashinsky equation is a nonlinear partial differential equation that can be used to describe traveling waves in dispersive media, such as plasma and porous media [11], and also the dynamics of flame propagation in turbulent combustion. It is a generalization of the Kuramoto–Sivashinsky equation, which exhibits chaotic behavior and arises in a wide range of physical systems [12]. The fractional generalized Kuramoto–Sivashinsky equation involves fractional derivatives with nonsingular kernels,

which can capture the memory and nonlocal effects of complex phenomena.

The fractional generalized Kuramoto–Sivashinsky equation is given by the following equation:

$$\mathscr{D}_{\text{ţ}}^{\alpha}\varphi + \varphi_{\xi}\varphi + \mu\varphi_{\xi\xi} + \vartheta\varphi_{\xi\xi\xi} + \delta\varphi_{\xi\xi\xi\xi} = 0, \quad 0 < \alpha \leqslant 1. \tag{1}$$

An electrostatic variable is denoted by $\varphi(\xi, \text{ţ})$, and the parameters μ, ϑ, and δ are coefficients that determine the strength of the second-, third-, and fourth-order derivatives, respectively. They can affect the stability and dynamics of the traveling waves. The parameter α is the fractional order of the time derivative, which can capture the memory and nonlocal effects of complex phenomena.

The GKSE models various phenomena in science and engineering, such as chemical reactions, flows, flames, and reaction-diffusion systems. It also occurs in ocean engineering problems, such as viscous flow, magneto hydrodynamics, weather and climate, microtide turbulence, and off-shore industry. The Kuramoto–Sivashinky equation (KSE) [13] is a special case of the generalized Kuramoto–Sivashinky (1) when $\mu = \delta = 1$ and $\vartheta = 0$. The Laplace transformation and the variational iteration method were used by Shah et al. to solve (1) [14]. The modified Kudrayshov method was used to solve (1) with $\mu = \delta = \vartheta = 1$ in [15]. The approximated solution of the KSE was analyzed by Veeresha and Prakasha using novel computational technique [16].

1.2. The Fractional Generalized Regularized Long Wave (FGRLW) Equation. A mathematical formula called the FGRLW equation is used to describe how small-amplitude extended waves travel through a fluid's surface, and it also describes the behavior of long water waves in the ocean, including their propagation and interaction with different coastal structures. So, it is suitable to investigate this equation in fractional derivative to predict any unusual formulation of waves. It can be stated as follows:

$$\mathscr{D}_{\text{ţ}}^{\alpha}\varphi + \varphi_{\xi} + a\varphi_{\xi}\varphi^{p} - \mu\varphi_{\xi\xi\text{ţ}} = 0, \quad 0 < \alpha \leqslant 1. \tag{2}$$

The FGRLW equation involves several parameters, including constant μ, a positive integer a, and the order α of the fractional derivative $D_{\text{ţ}}^{\alpha}$. These parameters determine the behavior of the system and its solutions. The term $\mathscr{D}_{\text{ţ}}^{\alpha}\varphi$ represents the time derivative of the dependent variable $\varphi(\xi, \text{ţ})$, while φ_{ξ} represents its spatial derivative. The term $\varphi_{\xi}\varphi^{p}$ is a nonlinear term that describes the effects of wave-wave interactions. Numerous disciplines, including fluid dynamics, plasma physics, and quantum mechanics, use the FGRLW equation extensively. Its solutions exhibit interesting phenomena such as solitary waves, which are waves that maintain their shape and speed over long distances. The study of the FGRLW equation and its solutions can provide insights into the behavior of complex systems and phenomena in nature.

When $p = 1$, the equation becomes the regularized long wave equation, which is a significant equation in physics media. It models phenomena that involve weak nonlinearity and dispersive waves equation [17]. When $p = 2$, the FGRLW becomes a special case that is called the modified regularized long wave (FMRLW) equation. Different approaches for solving the GRLW equation have been proposed in the literature. Nuruddeen et al. [18] introduced the METEM method for solving the FRLW equation. Nikan et al. used a finite difference method for solving the FRLW equation [19]. The optimal homotopy asymptotic method was presented by Nawaz et al. [20] for solution for the DGRLW equation. Also, there are many methods that have been used to solve this equation.

This paper intends to clarify the LRPS, a straightforward and successful technique for resolving differential equations with variable coefficients. The LRPS method was suggested in [21, 22] and provides a more straightforward and precise way to compute solutions for the equations mentioned earlier. We use the Laplace transform (LT) and power series method to deal with nonlinear differential equations. This involves changing the equations to Laplace space and using a suitable expansion to solve the equation that results from the power series method. To do this, we have created a new expansion that represents the solution of the equation in Laplace space. The coefficients of the series are then determined by the LRPS method. The LRPS method is simpler and more efficient than the conventional residual power series method, as it determines the coefficients based on the concept of the limit instead of on fractional derivation. This reduces the calculations, avoiding the need to repeatedly calculate fractional derivatives as required in the RPS method. Our suggested approach makes it possible to obtain precise and accurate approximations by adding a fast convergent series.

This paper consists of the following sections. In Section 1, we explain some important terms and ideas related to fractional calculus, and in Section 2, we present the specific type of fractional series that we will use in our study. Next, in Section 3, we describe the LRPS method, which is a useful technique for finding and predicting unique solutions to nonlinear fractional differential equations. Then, in Section 4, we demonstrate how the LRPS method works on two different differential equations. In addition, Section 5 shows graphs of the solutions that we obtained in Section 4. In Section 6, we discuss the results and their significance. Finally, we conclude by summarizing our main points and implications.

2. Preliminaries

Here, we introduce fundamental definitions and concepts of fractional calculus [23], alongside theorems related to Laplace transform [21].

Definition 1. If a real function $\varphi(\text{ţ})$, where $\text{ţ} > 0$, satisfies the condition that there exists a real number $\rho > \upsilon$ such that $\varphi(\text{ţ}) = \text{ţ}^{\rho}\varphi_1(\text{ţ})$, where $\varphi_1(\text{ţ}) \in \mathbb{C}(0, \infty)$, then it is said to belong to the space $\mathbb{C}\upsilon$, where $\upsilon \in \mathbb{R}$. Similarly, if it satisfies the same condition but with $\rho > \upsilon$ being a natural number, then it is said to belong to the space $\mathbb{C}^{\aleph}\upsilon$, where $\aleph \in \mathbb{N}$.

Definition 2. The fractional integral of R–L of order α, $\alpha > 0$ of a function $\varphi(\mathfrak{t})$ is defined as follows:

$$\begin{cases} J^{\alpha}\varphi(\mathfrak{t}) = \dfrac{1}{\Gamma(\alpha)}\displaystyle\int_0^{\mathfrak{t}} (\mathfrak{t}-\zeta)^{(\alpha-1)}\varphi(\zeta)d\zeta, \text{when } \alpha > 0, \mathfrak{t} > 0, \\ J^{0}\varphi(\mathfrak{t}) = \varphi(\mathfrak{t}). \end{cases} \tag{3}$$

Some properties of J^{α} are, for $\gamma, \alpha \geqslant 0, \upsilon \geqslant -1$, given by the following equation:

$$\begin{aligned} J^{\alpha}J^{\gamma}\varphi(\mathfrak{t}) &= J^{\alpha+\gamma}, \\ J^{\alpha}\,\mathfrak{t}^{\psi} &= \frac{\Gamma(\psi+1)}{\Gamma(\psi+\alpha+1)}\,\mathfrak{t}^{\psi+\alpha}. \end{aligned} \tag{4}$$

Definition 3. Caputo fractional derivative is defined as follows:

$$\mathscr{D}^{\alpha}\varphi(\mathfrak{t}) = J^{m-\alpha}\mathscr{D}^{m}\varphi(\mathfrak{t}) = \frac{1}{\Gamma(\alpha)}\int_0^{\mathfrak{t}} (\mathfrak{t}-\zeta)^{(m-\alpha-1)}\varphi^{m}(\zeta)\mathrm{d}\zeta, \tag{5}$$

for $m-1 < \alpha \leqslant m$, $m \in \mathbb{N}$, and $\mathfrak{t} > 0$.

Lemma 4. *If $m-1 < \alpha \leqslant m$, $m \in \mathbb{N}$, and $\varphi(\mathfrak{t}) \in \mathbb{C}_{-1}^{m}$,*

$$\begin{cases} \mathscr{D}^{\alpha}J^{\alpha}\varphi(\mathfrak{t}) = \varphi(\mathfrak{t}), \\ J^{\alpha}\mathscr{D}^{\alpha}\varphi(\mathfrak{t}) = \varphi(\mathfrak{t}) - \displaystyle\sum_{k=0}^{m-1}\varphi^{(k)}(0)\frac{\mathfrak{t}^{k}}{k!}. \end{cases} \tag{6}$$

For further details, see [23]. Because it permits the formulation of our work by incorporating traditional initial and boundary conditions, we adopt the Caputo fractional derivative.

Definition 5. Suppose we have a function $\varphi(\xi, \mathfrak{t})$ that is piecewise continuous on $I \times [0, \infty)$ and has an exponential order of δ. In this case, we can define the Laplace transform of $\varphi(\xi, \mathfrak{t})$, denoted by $\Phi(x, \mathfrak{S})$, as follows [24]:

$$\Phi(\xi, \mathfrak{S}) \equiv \mathfrak{L}[\varphi(\xi, \mathfrak{t})] = \int_0^{\infty} e^{-\mathfrak{S}\mathfrak{t}}\varphi(\xi, \mathfrak{t})\mathrm{d}\mathfrak{t}, \quad \mathfrak{S} > \sigma, \tag{7}$$

using inverse Laplace transform.

$$\varphi(\xi, \mathfrak{t}) \equiv \mathfrak{L}^{-1}[\varphi(\xi, \mathfrak{S})] = \frac{1}{2\pi i}\int_{\epsilon-i\infty}^{\epsilon+i\infty} e^{\mathfrak{S}\mathfrak{t}}\varphi(\xi, \mathfrak{S})\mathrm{d}\mathfrak{S}, \quad \epsilon > \epsilon_0. \tag{8}$$

The Laplace transform's integral converges absolutely only in the right half-plane, where ϵ_0 is located.

Lemma 6. *Suppose we have a piecewise continuous function $\varphi(\xi, \mathfrak{t})$ on $I \times [0, \infty)$, with its Laplace transform denoted by $\Phi(\xi, \mathfrak{S}) = \mathfrak{L}[\varphi(\xi, \mathfrak{t})]$. The function has the following characteristics:*

(1) $\mathfrak{L}\left\{1/\Gamma(\alpha)\int_0^{\mathfrak{t}} (\mathfrak{t}-\zeta)^{(\alpha-1)}\varphi(\xi, \zeta)\mathrm{d}\zeta\right\} = \mathfrak{S}^{\alpha-1}\Phi(\xi, \mathfrak{S})$, for $\alpha > 0$

(2) $\mathfrak{L}\left\{\mathscr{D}_{\mathfrak{t}}^{\alpha}\varphi(\xi, \mathfrak{t})\right\} = \mathfrak{S}^{\alpha}\Phi(\xi, \mathfrak{S}) - \sum_{k=0}^{m-1}\mathfrak{S}^{\alpha-k-1}\partial^{k}/\partial\mathfrak{t}^{k}\varphi(\xi, 0)$, for $m-1 < \alpha < m$

(3) $\mathfrak{L}\left\{\mathscr{D}_{\mathfrak{t}}^{n\alpha}\varphi(\xi, \mathfrak{t})\right\} = \mathfrak{S}^{n\alpha}\Phi(\xi, \mathfrak{S}) - \sum_{k=0}^{n-1}\mathfrak{S}^{(n-k)\alpha-1}\mathscr{D}_{\mathfrak{t}}^{k\alpha}\varphi(\xi, 0)$, for $0 < \alpha < 1$

Here, $D_{\mathfrak{t}}^{n\alpha} = \partial^{n}/\partial\mathfrak{t}^{n}(D_{\mathfrak{t}}^{\alpha})$ represents the Caputo derivative.

The demonstration for this lemma can be found in [25].

Theorem 7. *Consider a function $\varphi(\xi, \mathfrak{t})$ that is sequentially consistent on the interval I and for which the exponential order δ exists on the time interval $[0, \infty)$. Let $\Phi(\xi, \mathfrak{S})$ be the Laplace transform of $\varphi(\xi, \mathfrak{t})$. Suppose that the fractional expansion of $\Phi(\xi, \mathfrak{S})$ is given by the following equation:*

$$\Phi(\xi, \mathfrak{S}) = \sum_{n=0}^{\infty}\frac{\rho_n(\xi)}{\mathfrak{S}^{n\alpha+1}}, \quad 0 < \alpha \leqslant 1, \xi \in I, \mathfrak{S} > \xi, \tag{9}$$

then the coefficients $\rho_n(x)$ are equal to the nth derivative of $\varphi(\xi, \mathfrak{t})$ with respect to time evaluated at $\mathfrak{t} = 0$, denoted by $D_{\mathfrak{t}}^{n\alpha}\varphi(\xi, 0)$.

This theorem provides a useful tool for solving fractional differential equations and other mathematical problems involving the Laplace transform, particularly those with a fractional expansion. The evidence of theorem (1) can be found in [25].

Remark 8. It is stated that the inverse Laplace transform of the equation presented in (3) can be expressed in the following manner:

$$\varphi(\xi, \mathfrak{t}) = \sum_{n=0}^{\infty}\frac{D_{\mathfrak{t}}^{n\alpha}\varphi(\xi, 0)}{\Gamma(1+n\alpha)}\mathfrak{t}^{n\alpha}, \quad 0 < \alpha \leqslant 1, \mathfrak{t} \geq 0. \tag{10}$$

The fractional Taylor's formula, as described in [26], is associated with the expression given for the inverse Laplace transform.

3. An Overview of the LRPSM Methodology

Using LRPSM, which is a method for solving complex equations involving fractional derivatives, we will explore the basic concepts and techniques for dealing with nonlinear fractional PDEs, which are equations that describe phenomena with fractional order of change.

$$\mathscr{D}_{\mathfrak{t}}^{\alpha}\varphi(\xi, \mathfrak{t}) + \mu\Omega\varphi[(\xi, \mathfrak{t})] + \beta\Psi[\varphi(\xi, \mathfrak{t})] = 0, \quad 0 < \alpha \leqslant 1, \tag{11}$$

subject to

$$\varphi(\xi, 0) = \rho_0(\xi), \tag{12}$$

and the path of motion of a solitary wave is given by an unknown function $\varphi(\xi, \mathfrak{t})$ that depends on ξ and $\mathfrak{t}$. The

Caputo derivative is presented by $D_{\text{ţ}}^{\alpha}$, while μ and β are constant values. The functions Ω and Ψ can be either linear or nonlinear.

First, applying LT to equation (11), we have the following equation:

$$\text{Ţ}\left\{\mathscr{D}_{\text{ţ}}^{\alpha}\varphi(\xi,\text{ţ})\right\}+\mu\text{Ţ}\{\Omega[\varphi[\xi,\text{ţ}]]\}+\beta\text{Ţ}\{\Psi[\varphi(\xi,\text{ţ})]\}=0. \tag{13}$$

After applying the fact that $\text{Ţ}\left\{\mathscr{D}_{\text{ţ}}^{\alpha}\varphi(\xi,\text{ţ})\right\}=\mathfrak{S}^{\alpha}\Phi(\xi,\mathfrak{S})-\mathfrak{S}^{\alpha-1}\varphi(\xi,0)$ and using the initial condition (12), we can express equation (11) as follows:

$$\Phi(\xi,\mathfrak{S})-\frac{\rho_0(\xi)}{\mathfrak{S}}+\frac{\mu}{\mathfrak{S}^{\alpha}}\Omega[\Phi(\xi,\mathfrak{S})]+\frac{\beta}{\mathfrak{S}^{\alpha}}\text{Ţ}\left\{\Psi\text{Ţ}^{-1}[\Phi(\xi,\mathfrak{S})]\right\}=0, \tag{14}$$

where $\Phi(\xi,\mathfrak{S})=\text{Ţ}[\varphi(\xi,\text{ţ})]$.

Second, we express the function $\Phi(\xi,\mathfrak{S})$ that has been modified by a fractional Laplace transform as an infinite sum of terms.

$$\Phi(\xi,\mathfrak{S})=\sum_{n=0}^{\infty}\frac{\rho_n(\xi)}{\mathfrak{S}^{n\alpha+1}}. \tag{15}$$

Then, we write the function $\Phi_k(\xi,\mathfrak{S})$ that is the kth truncated of the series of (15) as follows:

$$\Phi_k(\xi,\mathfrak{S})=\sum_{n=0}^{k}\frac{\rho_n(\xi)}{\mathfrak{S}^{n\alpha+1}}=\frac{\rho_0(\xi)}{\mathfrak{S}}+\sum_{n=1}^{k}\frac{\rho_n(\xi)}{\mathfrak{S}^{n\alpha+1}}. \tag{16}$$

We define the LRF of (14) which is used to determine the unknown coefficients of the series in (16) by applying the LRPS method.

$$\begin{aligned}\text{Ţ}\mathrm{Res}(\xi,\mathfrak{S})&=\Phi(\xi,\mathfrak{S})-\frac{\rho_0(\xi)}{\mathfrak{S}}+\frac{\mu}{\mathfrak{S}^{\alpha}}\Omega[\Phi(\xi,\mathfrak{S})]\\&+\frac{\beta}{\mathfrak{S}^{\alpha}}\text{Ţ}\{\Psi\text{Ţ}[\Phi(\xi,\mathfrak{S})]\},\end{aligned} \tag{17}$$

and the kth LRF is as follows:

$$\begin{aligned}\text{Ţ}\mathrm{Res}_k(\xi,\mathfrak{S})&=\Phi_k(\xi,\mathfrak{S})-\frac{\rho_0(\xi)}{\mathfrak{S}}+\frac{\mu}{\mathfrak{S}^{\alpha}}\Omega\left[\Phi_k(\xi,\mathfrak{S})\right]\\&+\frac{\beta}{\mathfrak{S}^{\alpha}}\text{Ţ}\left\{\Psi\text{Ţ}^{-1}\left[\Phi_k(\xi,\mathfrak{S})\right]\right\}.\end{aligned} \tag{18}$$

Several properties that are present in the standard residual power series method [26] can also be extended to the LRPSM. These properties include the following properties:

(1) $\text{Ţ}\mathrm{Res}(\xi,\mathfrak{S})=0$ and $\lim_{k\longrightarrow\infty}\text{Ţ}\mathrm{Res}_k(\xi,\mathfrak{S})=\text{Ţ}\mathrm{Res}(\xi,\mathfrak{S})$ for $\mathfrak{S}>0$

(2) $\lim_{\mathfrak{S}\longrightarrow\infty}\mathfrak{S}\text{Ţ}\mathrm{Res}(\xi,\mathfrak{S})=0\Rightarrow\lim_{\mathfrak{S}\longrightarrow\infty}\mathfrak{S}\text{Ţ}\mathrm{Res}_k(\xi,\mathfrak{S})=0$

(3) $\lim_{\mathfrak{S}\longrightarrow\infty}\mathfrak{S}^{k\alpha+1}\text{Ţ}\mathrm{Res}(\xi,\mathfrak{S})=0=\lim_{\mathfrak{S}\longrightarrow\infty}\mathfrak{S}^{k\alpha+1}\text{Ţ}\mathrm{Res}_k(\xi,\mathfrak{S})=0,\ 0<\alpha\leqslant 1, k=1,2,3,4,\ldots$

We can recursively derive a system for obtaining the coefficient functions $\rho_n(\xi)$ by satisfying the following condition: $\lim_{\mathfrak{S}\longrightarrow\infty}\mathfrak{S}^{k\alpha+1}\text{Ţ}\mathrm{Res}_k(\xi,\mathfrak{S})=0,,,,,0<\alpha\leqslant 1, k=1,2,3,4,\ldots$

After obtaining the coefficient functions $\rho_n(\xi)$ through a recursive system, we use them to compute $\Phi_k(\xi,\mathfrak{S})$ for a given Laplace variable $\mathfrak{S}$ and then apply the inverse Laplace transform to obtain the kth approximate solution $\varphi_k(\xi,\text{ţ})$ as a function of the time variable ţ. This procedure allows us to solve the original problem using an iterative approach that yields increasingly accurate solutions with each iteration.

3.1. Convergence Analysis. Since the proposed technique lead to the truncated power series of the following form:

$$\sum_{\iota=0}^{\kappa}f_{\iota}=\sum_{\iota=0}^{\kappa}\varphi_{\iota}(\xi)\frac{\text{ţ}^{\iota\alpha}}{\Gamma(\iota\alpha+1)}, \tag{19}$$

with exact solution $\varphi_{\kappa}(\xi,\text{ţ})$, we can prove the convergence using the same manner as follows.

The investigated equation is written in the following form:

$$\mathscr{D}_{\text{ţ}}^{\alpha}\varphi(\xi,\text{ţ})=\mathrm{F}\left(\varphi,\varphi^2,\ldots,\varphi_x,\varphi_{xx},\ldots\right),\quad 0<\alpha\leq 1, \tag{20}$$

Theorem 9. *Let F be an operator from $H\longrightarrow H$ (where H is the Hilbert space) and let φ be the exact solution of equation (20), then the approximated solution (13) is convergent to φ if there exist a constant W, $(0<W\leq 1)$ in which $\|f_{\kappa+1}i(\xi,\text{ţ})\|\leq W\|f_{\kappa}i(\xi,\text{ţ})\|$, for all $\kappa\in N\cup\{0\}$.*

Proof. We aim to prove that $f_{\iota}\|_{\iota=0}^{\infty}$ is a convergent Cauchy sequence as follows:

$$\|f_{\iota+1}-f_{\iota}\|=\|f_{\iota+1}\|\leq B\|f_{\iota}\|\leq W^2\|f_{\iota-1}\|\leq\ldots\leq W^{\iota}\|f_1\|\leq W^{\iota+1}\|f_0\|. \tag{21}$$

For $\iota, m \in N, \iota > m$, we obtain the following equation:

$$\begin{aligned}\|f_\iota - f_m\| &= \|(f_\iota - f_{\iota-1}) + (f_{\iota-1} - f_{\iota-2}) + \cdots + (f_{m+1} - f_m)\| \\ &\leq \|(f_\iota - f_{\iota-1})\| + \|(f_{\iota-1} - f_{\iota-2})\| + \cdots + \|(f_{m+1} - f_m)\| \\ &\leq W^\iota \|f_0(\xi)\| + W^{\iota-1}\|\mathbf{f}_0(\xi)\| + \cdots + W^{m+1}\|\mathrm{f}_0(\xi)\| \\ &\leq \left(W^\iota + W^{\iota-1} + \cdots + W^{m+1}\right)\|\mathrm{f}_0(\xi)\| \\ &\leq W^{m+1}\frac{1 - W^{\iota-m}}{1 - W}\|\mathrm{f}_0(\xi)\| \longrightarrow 0 \text{ as } \iota,\ m \longrightarrow \infty.\end{aligned} \tag{22}$$

Hence, $f_\iota||_{\iota=0}^{\infty}$ is a convergent Cauchy sequence in H. □

4. Applications

We show how the LRPS method can find solitary solutions for some FPDEs that are common in many fields, such as the fractional generalized Kuramoto–Sivashinsky and fractional generalized regularized long wave equations. We give two examples to illustrate the advantages and performance of the LRPS method for these problems. We used MATHEMATICA 11 for all the symbolic and numerical computations in this paper.

4.1. Application 1. Given the following, the fractional generalized Kuramoto–Sivashinsky equation is as follows:

$$\mathscr{D}_{\text{ţ}}^{\alpha}\varphi + \varphi_\xi\varphi + \mu\varphi_{\xi\xi} + \vartheta\varphi_{\xi\xi\xi} + \delta\varphi_{\xi\xi\xi\xi} = 0, \quad 0 < \alpha \leqslant 1, \tag{23}$$

with initial condition

$$\varphi(\xi, 0) = \Omega(\xi). \tag{24}$$

4.1.1. Case I. Let us consider FKS (23) for $\mu = -1, \vartheta = 0, \delta = 1$ [16]:

$$\mathscr{D}_{\text{ţ}}^{\alpha}\varphi + \varphi_\xi\varphi - \varphi_{\xi\xi} + \varphi_{\xi\xi\xi\xi} = 0, \tag{25}$$

with initial condition

$$\varphi(\xi, 0) = \beta + \frac{15\tan h^3[\kappa(\xi - \nu)] - 45\tan h[\kappa(\xi - \nu)]}{19\sqrt{19}}, \tag{26}$$

where β, ν, and κ are constants. The exact solution at $\alpha = 1$ is as follows:

$$\varphi(\xi, \text{ţ}) = \beta + \frac{15\tan h^3[\kappa(\xi - \beta\text{ţ} - \nu)] - 45\tan h[\kappa(\xi - \beta\text{ţ} - \nu)]}{19\sqrt{19}}. \tag{27}$$

We apply the LT on equation (25) and the initial condition from equation (26) to obtain the following equation:

$$\Phi(\xi, \mathfrak{S}) - \frac{\varphi(\xi, 0)}{\mathfrak{S}} + \frac{1}{\mathfrak{S}^\alpha}\text{Ţ}\left[\text{Ţ}^{-1}\left[\Phi(\xi, \mathfrak{S})_\xi\right]\text{Ţ}^{-1}[\Phi(\xi, \mathfrak{S})]\right] + \frac{1}{\mathfrak{S}^\alpha}\left[(-\Phi(\xi, \mathfrak{S}))_{\xi\xi} + (\Phi(\xi, \mathfrak{S}))_{\xi\xi\xi\xi}\right] = 0. \tag{28}$$

We presume that the following form is the series solution of equation (25):

$$\Phi(\xi, \mathfrak{S}) = \sum_{n=0}^{\infty}\frac{\rho_n(\xi)}{\mathfrak{S}^{n\alpha+1}}. \tag{29}$$

The kth truncate series of equation (25) can be obtained by performing the following steps:

$$\Phi_k(\xi, \mathfrak{S}) = \frac{\rho_0(\xi)}{\mathfrak{S}} + \sum_{n=1}^{k}\frac{\rho_n(\xi)}{\mathfrak{S}^{n\alpha+1}}. \tag{30}$$

Furthermore, we provide the following description for the kth LRF of equation (25):

$$\text{Ţ}\text{Res}_k(\xi, \mathfrak{S}) = \Phi_k(\xi, \mathfrak{S}) - \frac{\varphi(\xi, 0)}{\mathfrak{S}} + \frac{1}{\mathfrak{S}^\alpha}\text{Ţ}\left[\text{Ţ}^{-1}\left[\Phi_k(\xi, \mathfrak{S})_\xi\right]\text{Ţ}^{-1}[\Phi_k(\xi, \mathfrak{S})]\right] + \frac{1}{\mathfrak{S}^\alpha}\left[-(\Phi_k(\xi, \mathfrak{S}))_{\xi\xi} + (\Phi_k(\xi, \mathfrak{S}))_{\xi\xi\xi\xi}\right]. \tag{31}$$

To find $\rho_k(\xi)$ for $k = 1, 2, 3, \ldots$, we begin by substituting the kth truncate series (31) into the kth LRF equation (31). We then multiply both sides of (31) by $\mathfrak{S}^{k\alpha+1}$. Next, we solve the resulting relation $\lim_{\mathfrak{S}\longrightarrow\infty}\mathfrak{S}^{k\alpha+1}\text{Ţ}\text{Res}_k(\xi, \mathfrak{S}) = 0, k = 1, 2, 3, 4, \ldots$ recursively to obtain $\rho_k(\xi)$. We can now obtain the first few elements of the sequence $\rho_k(\xi)$.

$$\rho_0(\xi) = \beta + \frac{15\tan h^3[\kappa(\xi - \nu)] - 45\tan h[\kappa(\xi - \nu)]}{19\sqrt{19}},$$

$$\begin{aligned}
\rho_1(\xi) = {} & -\frac{1}{27436}45\kappa\sec h^7[\kappa(-\nu + \xi)](-57\sqrt{19}\beta\cos h[\kappa(-\nu + \xi)] \\
& - 19\sqrt{19}\beta\cos h[3\kappa(-\nu + \xi)] + 430 - 38\sqrt{19}\kappa - 1672\sqrt{19}\kappa^3 \\
& + \left(15 - 38\sqrt{19}\kappa + 608\sqrt{19}\kappa^3\right)\cos h[2\kappa(-\nu + \xi)]\sin h[\kappa(-\nu + \xi)],
\end{aligned}$$

$$\begin{aligned}
\rho_2(\xi) = {} & \frac{1}{139129348431872}45k^2\sec h^{20}[k(-\nu + \xi)] \\
& \cdot 162362880000\sqrt{19}k^3 - 4491417600000k^4 \\
& + 2275651584000\sqrt{19}k^5 - 596460257280000k^6 + 336796434432000\sqrt{19}k^7 \\
& + 32532715044864000\sqrt{19}k^9 + 308868589260\beta - 403653658980\sqrt{19}k\beta \\
& - 16891353114240\sqrt{19}k^3\beta - 213342336000\sqrt{19}k^3\beta^2 - 20\left(2245708800k^4 - 39823902720\sqrt{19}k^5\right) \\
& - 31969910476800k^6 + 5711885475840\sqrt{19}k^7 \\
& + 2212661548154880\sqrt{19}k^9 - 24349957566\beta + 33637804915\sqrt{19}k\beta \\
& + 8\sqrt{19}k^3\left(688176000 + 158873940137\beta + 1688960160\beta^2\right)\cosh[2k(-\nu + \xi)] + \ldots.
\end{aligned} \tag{32}$$

We can write the solution of (25) using the LRPS method as an infinite series.

$$\Phi(\xi, \mathfrak{S}) = \frac{\rho_0(\xi)}{\mathfrak{S}} + \frac{\rho_1(\xi)}{\mathfrak{S}^{\alpha+1}} + \frac{\rho_2(\xi)}{\mathfrak{S}^{2\alpha+1}} + \ldots. \tag{33}$$

The kth-approximate solution of our problem is obtained by taking the Laplace inverse of (33):

$$\varphi(\xi, \text{ţ}) = \rho_0(\xi) + \frac{\rho_1(\xi)\text{ţ}^{\alpha}}{\Gamma(\alpha + 1)} + \frac{\rho_2(\xi)\text{ţ}^{2\alpha}}{\Gamma(2\alpha + 1)} + \ldots. \tag{34}$$

We have the option to compute additional coefficients; however, we will limit our calculation to ρ_2. We will then compare the errors between the exact solution and the approximate solution obtained from this series.

Table 1 presents the results obtained by applying the LRPS method to solve the FKS equation (25) (Case I) for different combinations of time (ţ), spatial variable (ξ), and fractional derivative order (α). It demonstrates the convergence of solutions for different values of α.

Table 1: Numerical results for FGKS equation (25) of case (I) at $\beta = 5, \kappa = 1/2\sqrt{19}, \nu = -25$ and difference values of α.

ţ	ξ	$\alpha = 0.6$	$\alpha = 0.75$	$\alpha = 0.95$
1.5	−5	4.63869	4.63871	4.63873
	−4	4.63835	4.63837	4.63838
	−3	4.63814	4.63815	4.63815
	5	4.63777	4.63777	4.63777
2	−5	4.63882	4.63889	4.63896
	−4	4.63844	4.63848	4.63853
	−3	4.63819	4.63822	4.63825
	5	4.63778	4.63778	4.63778

4.1.2. Case II. Let us consider the FKS (25) for $\mu = 1, \vartheta = 0, \delta = 1$ [16]:

$$\mathscr{D}_{ţ}^{\alpha}\varphi + \varphi_{\xi}\varphi + \varphi_{\xi\xi} + \varphi_{\xi\xi\xi\xi} = 0, \tag{35}$$

with initial state

$$\varphi(\xi, 0) = \beta + \frac{15}{19}\sqrt{\frac{11}{19}}\left(11\tan h^{3}(\kappa(\xi - \nu)) - 9\tanh(\kappa(\xi - \nu))\right). \tag{36}$$

where β, ν, and κ are constants.The exact solution at $\alpha = 1$ is

$$\varphi(\xi, ţ) = \beta + \frac{15}{19}\sqrt{\frac{11}{19}}\left(11\tan h^{3}(\kappa(\xi - \beta ţ - \nu)) - 9\tanh(\kappa(\xi - \beta ţ - \nu))\right). \tag{37}$$

By performing a LT on both sides of equation (35) and utilizing the initial condition provided in equation (36), we can derive the following expression:

$$\Phi(\xi, \mathfrak{S}) - \frac{\varphi(\xi, 0)}{\mathfrak{S}} + \frac{1}{\mathfrak{S}^{\alpha}}Ł\left[Ł^{-1}\left[\Phi(\xi, \mathfrak{S})_{\xi}\right]Ł^{-1}[\Phi(\xi, \mathfrak{S})]\right] + \frac{1}{\mathfrak{S}^{\alpha}}\left[(\Phi(\xi, \mathfrak{S}))_{\xi\xi} + (\Phi(\xi, \mathfrak{S}))_{\xi\xi\xi\xi}\right] = 0. \tag{38}$$

We make the assumption that the series solution of equation (35) takes the following form:

$$\Phi(\xi, \mathfrak{S}) = \sum_{n=0}^{\infty}\frac{\rho_n(\xi)}{\mathfrak{S}^{n\alpha+1}}. \tag{39}$$

The kth truncated series of equation (35) can be obtained by the following equation:

$$\Phi_k(\xi, \mathfrak{S}) = \frac{\rho_0(\xi)}{\mathfrak{S}} + \sum_{n=1}^{k}\frac{\rho_n(\xi)}{\mathfrak{S}^{n\alpha+1}}. \tag{40}$$

We can define the kth LRF of equation (35) in the following manner:

$$\begin{aligned} Ł\text{Res}_k(\xi, \mathfrak{S}) = \Phi_k(\xi, \mathfrak{S}) - \frac{\varphi(\xi, 0)}{\mathfrak{S}} + \frac{1}{\mathfrak{S}^{\alpha}}Ł\left[Ł^{-1}\left[\Phi_k(\xi, \mathfrak{S})_{\xi}\right]Ł^{-1}\left[\Phi_k(\xi, \mathfrak{S})\right]\right] \\ + \frac{1}{\mathfrak{S}^{\alpha}}\left[(\Phi_k(\xi, \mathfrak{S}))_{\xi\xi} + 4(\Phi(\xi, \mathfrak{S}))_{\xi\xi\xi} + (\Phi_k(\xi, \mathfrak{S}))_{\xi\xi\xi\xi}\right]. \end{aligned} \tag{41}$$

To find $\rho_k(\xi)$ for $k = 1, 2, 3, \ldots$, we begin by substituting the kth truncate series (40) into the kth LRF (41). We then multiply both sides of equation (41) by $\mathfrak{S}^{k\alpha+1}$. Next, we solve the resulting relation $\lim_{\mathfrak{S}\longrightarrow\infty}\mathfrak{S}^{k\alpha+1}Ł\mathit{Res}_k(\xi, \mathfrak{S}) = 0, k = 1, 2, 3, 4, \ldots$ recursively to obtain $\rho_k(\xi)$. We can now obtain the first few elements of the sequence $\rho_k(\xi)$.

$$\begin{aligned}
\rho_0(\xi) &= \beta + \frac{15}{19}\sqrt{\frac{11}{19}}\left(11\tan h^3(\kappa(\xi-\nu)) - 9\tan h(\kappa(\xi-\nu))\right),\\
\rho_1(\xi) &= -\frac{1}{27436}45\kappa\sec h^7\kappa(-\nu+\xi)\\
&\quad(-57\sqrt{19}\beta\cosh(\kappa(-\nu+\xi)) - 19\sqrt{19}\beta\cosh(3\kappa(-\nu+\xi)))\\
&\quad-\frac{180}{27436}\kappa\sec h^7\kappa(-\nu+\xi)\sin h\kappa(-\nu+\xi)\\
&\quad\cdot\left(30 - 38\sqrt{19}\kappa - 1672\sqrt{19}\kappa^3 + \left(15 - 38\sqrt{19}\kappa + 608\sqrt{19}\kappa^3\right)\cosh(2\kappa(-\nu+\xi))\right),\\
\rho_2(\xi) &= \frac{45\kappa^2\sec h^{20}(\kappa(\xi-\nu))}{139129348431872}\left(-14086852217856000\sqrt{209}\kappa^5 - 2195584579584000000\kappa^4\right)\\
&\quad- 1176121279618560000\sqrt{209}\kappa^3 + 63274008537501696000\kappa^6 + 61497533769540\beta\\
&\quad+ 2952744405000192000\sqrt{209}\kappa^7 - 407623914461085696000\sqrt{209}\kappa^9\\
&\quad+ 3094678052180\sqrt{209}\beta\kappa - 157818230567360\sqrt{209}\beta\kappa^3 + 456054800256000\sqrt{209}\beta^2\kappa^3\\
&\quad+ 176\left(8898688491264000\kappa^4 + 1984083724800\sqrt{209}\kappa^5 - 5476943044260864000\kappa^6\right)\\
&\quad- 11205934203801600\sqrt{209}\kappa^7 + 3478774808768716800\sqrt{209}\kappa^9 + 477602355615\beta +\\
&\quad\cdot 28745033291\sqrt{209}\beta\kappa + 8\sqrt{209}\left(215120188800\beta^2 - 166024914049\beta + 1289172289680000\right)\\
&\quad\cdot\kappa^3\cosh(2\kappa(\xi-\nu)) - \ldots.
\end{aligned} \tag{42}$$

The solution to (35) via the LRPS method can be expressed as an infinite series.

$$\Phi(\xi,\mathfrak{S}) = \frac{\rho_0(\xi)}{\mathfrak{S}} + \frac{\rho_1(\xi)}{\mathfrak{S}^{\alpha+1}} + \frac{\rho_2(\xi)}{\mathfrak{S}^{2\alpha+1}} + \ldots. \tag{43}$$

By applying Laplace inverse to (43), we can obtain the kth-approximate solution to our problem.

$$\varphi(\xi,\text{ţ}) = \rho_0(\xi) + \frac{\rho_1(\xi)\text{ţ}^{\alpha}}{\Gamma(\alpha+1)} + \frac{\rho_2(\xi)\text{ţ}^{2\alpha}}{\Gamma(2\alpha+1)} + \ldots. \tag{44}$$

We could calculate more coefficients, but for now, we will only calculate ρ_2. Afterward, we will compare the errors between the precise solution and the estimated solution obtained from this series.

Table 2 presents the results obtained by applying the LRPS method to solve the FKS equation (35) (Case II) for different combinations of time (ţ), spatial variable (ξ), and fractional derivative order (α). It demonstrates the convergence of solutions for different values of α.

4.1.3. Case III. Let us consider FKS (16) for $\mu = 1, \vartheta = 4, \delta = 1$ [16]:

$$\mathcal{D}_{\text{ţ}}^{\alpha}\varphi + \varphi_{\xi}\varphi + \varphi_{\xi\xi} + 4\vartheta\varphi_{\xi\xi\xi} + \varphi_{\xi\xi\xi\xi} = 0, \tag{45}$$

with initial condition

$$\varphi(\xi,0) = \beta + 9 - 15\left(-\tan h^3(\kappa(\xi-\beta\text{ţ}-\nu)) + \tan h^2(\kappa(\xi-\beta\text{ţ}-\nu)) + \tan h(\kappa(\xi-\nu))\right), \tag{46}$$

where β, ν, and κ are constants. The exact solution at $\alpha = 1$ is

Table 2: Numerical results for FGKS equation of case (II) (35) at $\beta = 5, \kappa = 0.5\sqrt{11/19}, \nu = -25$ and difference values of α.

ţ	ξ	$\alpha = 0.6$	$\alpha = 0.75$	$\alpha = 0.95$
1.5	−5	6.201210	6.201200	6.201220
	−4	6.201310	6.201310	6.201310
	−3	6.201360	6.201360	6.201360
	5	6.201400	6.201400	6.201400
2	−5	6.201090	6.201080	6.201100
	−4	6.201250	6.201250	6.201260
	−3	6.201330	6.201330	6.201330
	5	6.201400	6.201400	6.201400

$$\varphi(\xi, ţ) = \beta + 9 - 15\left(-\tan h^3(\kappa(\xi - \nu)) + \tan h^2(\kappa(\xi - \beta ţ - \nu)) + \tan h(\kappa(\xi - \beta ţ - \nu))\right). \tag{47}$$

Following the initial condition specified in equation (46) while performing the Laplace transform of each side of equation (45), we obtain the following equation:

$$\Phi(\xi, \mathfrak{S}) - \frac{\varphi(\xi, 0)}{\mathfrak{S}} + \frac{1}{\mathfrak{S}^{\alpha}} Ľ\left[Ľ^{-1}\left[\Phi(\xi, \mathfrak{S})_{\xi}\right] Ľ^{-1}[\Phi(\xi, \mathfrak{S})]\right] - \frac{1}{\mathfrak{S}^{\alpha}}\left[(\Phi(\xi, \mathfrak{S}))_{\xi\xi} + (\Phi(\xi, \mathfrak{S}))_{\xi\xi\xi\xi}\right] = 0. \tag{48}$$

We presume that the following form can be used to express the series answer of equation (45):

$$\Phi(\xi, \mathfrak{S}) = \sum_{n=0}^{\infty} \frac{\rho_n(\xi)}{\mathfrak{S}^{n\alpha+1}}. \tag{49}$$

The kth truncated series of equation (45) can be obtained by performing the following steps:

$$\Phi_k(\xi, \mathfrak{S}) = \frac{\rho_0(\xi)}{\mathfrak{S}} + \sum_{n=1}^{k} \frac{\rho_n(\xi)}{\mathfrak{S}^{n\alpha+1}}. \tag{50}$$

Furthermore, we provide the following definition for the kth LRF of equation (45):

$$\begin{aligned} Ľ\mathrm{Res}_k(\xi, \mathfrak{S}) = \Phi_k(\xi, \mathfrak{S}) - \frac{\varphi(\xi, 0)}{\mathfrak{S}} + \frac{1}{\mathfrak{S}^{\alpha}} Ľ\left[Ľ^{-1}\left[\Phi_k(\xi, \mathfrak{S})_{\xi}\right] Ľ^{-1}[\Phi_k(\xi, \mathfrak{S})]\right] \\ + \frac{1}{\mathfrak{S}^{\alpha}}\left[(\Phi_k(\xi, \mathfrak{S}))_{\xi\xi} + 4(\Phi(\xi, \mathfrak{S}))_{\xi\xi\xi} + (\Phi_k(\xi, \mathfrak{S}))_{\xi\xi\xi\xi}\right]. \end{aligned} \tag{51}$$

In order to compute $\rho_k(\xi)$ for values of k from 1 to infinity, we first insert the truncated series expression (50) for the kth term into the corresponding LRF (51). We then multiply equation (51) by $\mathfrak{S}^{k\alpha+1}$ and proceed to solve the resulting equation:

$$\lim_{\mathfrak{S} \longrightarrow \infty} \mathfrak{S}^{k\alpha+1} Ľ\mathrm{Res}_k(\xi, \mathfrak{S}) = 0, \quad k = 1, 2, 3, 4, \ldots, \tag{52}$$

recursively to determine $\rho_k(\xi)$.

By following this method, we are able to calculate the initial terms of the sequence $\rho_k(\xi)$ as follows:

$$\begin{aligned}
\rho_0(\xi) &= \beta + 9 - 15\left(-\tan h^3(\kappa(\xi - \beta ṭ - v)) + \tan h^2(\kappa(\xi - \beta ṭ - v)) + \tan h(\kappa(\xi - v))\right),\\
\rho_1(\xi) &= \frac{1}{8}(-15)ksech^6(k(\xi - v))\left(4\left(\beta + 344k^3 - 32k^2 + 2k - 36\right)\right)\\
&\quad \cdot \cos h(2k(\xi - v)) + \left(\beta - 136k^3 + 112k^2 - 10k - 6\right)\cos h(4k(\xi - v))\\
&\quad + 3\left(\beta - 456k^3 - 80k^2 + 2\left(\beta + 120k^3 - 112k^2 - 2k + 14\right)\sin h(2k(\xi - v))\right.\\
&\quad + \left(\beta - 40k^3 + 48k^2 - 2k - 6\right)\sin h(4k(\xi - v)) + 6k + 74\\
&\quad + \left(\beta - 40k^3 + 48k^2 - 2k - 6\right)\sinh(4k(\xi - v))(\tanh(k(\xi - v)) - 1),\\
\rho_2(\xi) &= \frac{15k^2 \sec h^{20}(k(\xi - v))(\cosh(k(\xi - v)) - \sinh(k(\xi - v)))}{32768}\\
&\quad \cdot \left(10\left(282805862400k^9 + 1756448686080k^8 - 55526031360k^7\right)\right)\\
&\quad + 267156 - 3289\beta^2 - 37752\beta + 352(949\beta + 192)k^2 + 22(559\beta + 7986)k\\
&\quad \cdot 256(2980800\beta - 729836371)k^5 - 2752(2851200\beta + 190438387)k^6 \ldots\\
&\quad \cdot \cosh(k(\xi - v)) - 8\left(656985600000k^9 + 3528382464000k^8 - 99503769600k^7\right)\\
&\quad - 352(637\beta - 447)k^2 - 11(1001\beta + 10344)k + +80(702000\beta + 88825831)k^4\\
&\quad + 128(9082800\beta - 3024200401)k^5 + \ldots \cosh(3k(\xi - v)) \ldots.
\end{aligned} \tag{53}$$

We can write the solution of (45) using the LRPS method as an infinite series.

$$\Phi(\xi, \mathfrak{S}) = \frac{\rho_0(\xi)}{\mathfrak{S}} + \frac{\rho_1(\xi)}{\mathfrak{S}^{\alpha+1}} + \frac{\rho_2(\xi)}{\mathfrak{S}^{2\alpha+1}} + \ldots. \tag{54}$$

We can obtain the kth approximate solution to our problem by utilizing LI on equation (54).

$$\varphi(\xi, ṭ) = \rho_0(\xi) + \frac{\rho_1(\xi) ṭ^{\alpha}}{\Gamma(\alpha + 1)} + \frac{\rho_2(\xi) ṭ^{2\alpha}}{\Gamma(2\alpha + 1)} + \ldots. \tag{55}$$

For now, our main goal is to find the value of ρ_2. We might compute more coefficients later. Then, we will measure the differences between the exact solution and the approximation from this series. This allows us to assess the quality of the estimated solution.

Table 3 presents the results obtained by applying the LRPS method to solve the FKS equation (45) (Case III) for different combinations of time ($ṭ$), spatial variable (ξ), and fractional derivative order (α). It demonstrates the convergence of solutions for different values of α.

4.2. Application 2. Given the following time-fractional GRLWE,

$$\mathscr{D}_{ṭ}^{\alpha}\varphi + \varphi_{\xi} + a\varphi_{\xi}\varphi^{p} - \mu\varphi_{\xi\xi ṭ} = 0, \quad 0 < \alpha \leqslant 1,\ ṭ \geqslant 0, \xi \in \mathfrak{R}, \tag{56}$$

where p, a, and μ are real parameters.

With initial condition,

$$\varphi(\xi, 0) = \left(A\operatorname{csec} h^2\left(\frac{p}{2}\sqrt{\frac{\mathfrak{c}}{\mu(\mathfrak{c} + 1)}}(\xi - \xi_0)\right)\right)^{1/p}, \tag{57}$$

where $\mathfrak{c}, A$, and ξ_0 are constants. The exact solution is as follows:

$$\varphi(\xi, ṭ) = \left(A\operatorname{csec} h^2\left(\frac{p}{2}\sqrt{\frac{\mathfrak{c}}{\mu(\mathfrak{c} + 1)}}(\xi - (\mathfrak{c} + 1)ṭ - \xi_0)\right)\right)^{1/p}. \tag{58}$$

The parameters A and p are usually related to the amplitude and the phase of the wave packet, respectively. The parameter $\mathfrak{c}$ represents the speed of the wave packet, and $ṭ$ is the time variable. The parameter μ is related to the dispersion of the medium, and ξ_0 is the position of the wave packet's peak at time $ṭ = 0$.

4.2.1. Case I. When $p = 1$, the equation becomes the regularized long wave equation, which is a significant equation in physics media.

Given the following time-fractional RLWE,

$$\mathscr{D}_{ṭ}^{\alpha}\varphi + \varphi_{\xi} + \varphi_{\xi}\varphi - \varphi_{\xi\xi ṭ} = 0, \quad 0 < \alpha \leqslant 1. \tag{59}$$

The initial condition according to [27] is as follows:

Table 3: Numerical results for FGKS equation (45) of case (III) at $\beta = 3, \kappa = 0.5, \nu = -13$ and difference values of α.

ţ	ξ	$\alpha = 0.6$	$\alpha = 0.75$	$\alpha = 0.95$
1.5	−5	−2.99888	−2.99884	−2.99892
	−4	−2.99985	−2.99984	−2.99985
	−3	−2.99998	−2.99998	−2.99998
	5	−3.00000	−3.00000	−3.00000
2	−5	−2.99809	−2.99801	−2.99815
	−4	−2.99974	−2.99973	−2.99975
	−3	−2.99996	−2.99996	−2.99997
	5	−3.00000	−3.00000	−3.00000

$$\varphi(\xi, 0) = \left(3\mathfrak{c}\sec h^2\left(\frac{1}{2}\sqrt{\frac{\mathfrak{c}}{\mu(\mathfrak{c}+1)}}(\xi - \xi_0)\right)\right). \tag{60}$$

For $\alpha = 1$, the exact solution is as follows:

$$\varphi(\xi, ţ) = \left(3\mathfrak{c}\sec h^2\left(\frac{1}{2}\sqrt{\frac{\mathfrak{c}}{\mu(\mathfrak{c}+1)}}(\xi - (\mathfrak{c}+1)ţ - \xi_0)\right)\right). \tag{61}$$

After performing the LT on each sides of equation (59) and applying the initial condition described in equation (60), we can derive the following expression:

$$\Phi(\xi, \mathfrak{S}) - \frac{\varphi(\xi, 0)}{\mathfrak{S}} + \frac{1}{\mathfrak{S}^{\alpha}}\mathfrak{L}\left[\Phi(\xi, \mathfrak{S})_{\xi}\right] + \frac{a}{\mathfrak{S}^{\alpha}}Ł\left[Ł^{-1}\left[\Phi(\xi, \mathfrak{S})_{\xi}\right]Ł^{-1}\left[\Phi(\xi, \mathfrak{S})\right]\right] - \frac{\mu}{\mathfrak{S}^{\alpha}}\mathfrak{L}\left[\Phi(\xi, \mathfrak{S})_{\xi}\right] = 0. \tag{62}$$

We assume that the structure is taken by the series solution of equation (59):

$$\Phi(\xi, \mathfrak{S}) = \sum_{n=0}^{\infty}\frac{\rho_n(\xi)}{\mathfrak{S}^{n\alpha+1}}, \tag{63}$$

and the kth truncated series of equation (59) is obtained by the following equation:

$$\Phi_k(\xi, \mathfrak{S}) = \frac{\rho_0(\xi)}{\mathfrak{S}} + \sum_{n=1}^{k}\frac{\rho_n(\xi)}{\mathfrak{S}^{n\alpha+1}}. \tag{64}$$

To further clarify, we can define the kth LRF of equation (59) with the following formulation:

$$\begin{aligned} Ł\mathrm{Res}_k(\xi, \mathfrak{S}) = {} & \Phi_k(\xi, \mathfrak{S}) - \frac{\varphi(\xi, 0)}{\mathfrak{S}} - \frac{1}{2\mathfrak{S}^{\alpha}}Ł\left[Ł^{-1}\left[\Phi_k(\xi, \mathfrak{S})_{\xi\xi}\right]Ł^{-1}\left[\Phi_k(\xi, \mathfrak{S})\right]\right] \\ & + \frac{2}{\mathfrak{S}^{\alpha}}Ł\left[Ł^{-1}\left[\Phi_k(\xi, \mathfrak{S})_{\xi}\right]\left(Ł^{-1}\left[\Phi_k(\xi, \mathfrak{S})\right]\right)^2\right] - \frac{1}{\mathfrak{S}^{\alpha}}Ł\left[\left(Ł^{-1}\left[\Phi_k(\xi, \mathfrak{S})\right]\right)^2\right] = 0. \end{aligned} \tag{65}$$

To compute the values of $\rho_k(\xi)$ for k ranging from 1 to infinity, we employ a recursive method that involves inserting the truncated series expression (64) into the corresponding Laplace residual function (65). We then multiply the resulting equation by $\mathfrak{S}^{k\alpha+1}$ and solve for $\lim_{\mathfrak{S}\longrightarrow\infty}\mathfrak{S}^{k\alpha+1}Ł\mathrm{Res}_k(\xi, \mathfrak{S}) = 0, k = 1, 2, 3, 4, \ldots$ in a recursive manner to determine $\rho_k(\xi)$. By using this approach, we can calculate the initial terms of the sequence $\rho_k(\xi)$ without having to compute the entire infinite series.

$$\rho_0(\xi) = \left(3\mathfrak{c}\,\mathrm{sech}^2\left(\frac{1}{2}\sqrt{\frac{\mathfrak{c}}{\mu(\mathfrak{c}+1)}}(\xi-\xi_0)\right)\right),$$

$$\rho_1(\xi) = \frac{3}{2}\mathfrak{c}\sqrt{\frac{\mathfrak{c}}{\mathfrak{c}\mu+\mu}}\left(\cosh\left(\sqrt{\frac{\mathfrak{c}}{\mathfrak{c}\mu+\mu}}(\xi-\xi_0)\right)+12\mathfrak{c}+1\right)$$
$$\tanh\left(\frac{1}{2}\sqrt{\frac{\mathfrak{c}}{\mathfrak{c}\mu+\mu}}(\xi-\xi_0)\right)\mathrm{sech}^4\left(\frac{1}{2}\sqrt{\frac{\mathfrak{c}}{\mathfrak{c}\mu+\mu}}(\xi-\xi_0)\right),$$

$$\rho_2(\xi) = \frac{1}{32(\mathfrak{c}+1)\mu}\left(3\mathfrak{c}^2\left(-576\mathfrak{c}^2-96\mathfrak{c}-8+\left(432\mathfrak{c}^2-48\mathfrak{c}-9\right)\cosh\left(\sqrt{\frac{\mathfrak{c}}{\mathfrak{c}\mu+\mu}}(\xi-\xi_0)\right)+48\mathfrak{c}\cosh\left(2\sqrt{\frac{\mathfrak{c}}{\mathfrak{c}\mu+\mu}}(\xi-\xi_0)\right)+\cosh\left(3\sqrt{\frac{\mathfrak{c}}{\mathfrak{c}\mu+\mu}}(\xi-\xi_0)\right)\right)\mathrm{sech}^8\left(\frac{1}{2}\sqrt{\frac{\mathfrak{c}}{\mathfrak{c}\mu+\mu}}(\xi-\xi_0)\right)\right). \tag{66}$$

We can write the solution of (59) using the LRPS method as an infinite series.

$$\Phi(\xi,\mathfrak{S}) = \frac{\rho_0(\xi)}{\mathfrak{S}}+\frac{\rho_1(\xi)}{\mathfrak{S}^{\alpha+1}}+\frac{\rho_2(\xi)}{\mathfrak{S}^{2\alpha+1}}+\cdots. \tag{67}$$

By utilizing the Laplace inverse on equation (67), we can obtain an approximate solution to our problem for the kth iteration.

$$\varphi(\xi,\mathfrak{t}) = \rho_0(\xi)+\frac{\rho_1(\xi)\mathfrak{t}^{\alpha}}{\Gamma(\alpha+1)}+\frac{\rho_2(\xi)\mathfrak{t}^{2\alpha}}{\Gamma(2\alpha+1)}+\cdots. \tag{68}$$

Our primary purpose is to compute the numerical value of the third coefficient, ρ_2. Additional coefficients may need to be computed at a later time. Following that, we will carefully examine any inconsistencies between the exact solution and the estimated solution produced from this series. This will allow us to assess the precision and reliability of the calculated solution.

Table 4 displays the results of solving FRLW equation (59) using the LRPS method for different values of $\mathfrak{t}$ and ξ, as well as various values of α (namely, $\alpha = 0.6, 075$ and 1). We notice from the results of the table a convergence of solutions at different values of α.

4.2.2. Case II. When $p = 2$, the FGRLW becomes a special case that is called the modified regularized long wave (FMRLW) equation. Given the following time-fractional RLWE,

$$\mathscr{D}^{\alpha}_{\mathfrak{t}}\varphi+\varphi_{\xi}+6\varphi_{\xi}\varphi^2-\mu\varphi_{\xi\xi\mathfrak{t}} = 0, \quad 0<\alpha\leqslant 1. \tag{69}$$

The initial condition according to [28] is

$$\varphi(\xi,0) = \left(\sqrt{\mathfrak{c}}\,\mathrm{sec}\,h\left(\sqrt{\frac{\mathfrak{c}}{\mu(\mathfrak{c}+1)}}(\xi-\xi_0)\right)\right). \tag{70}$$

For $\alpha = 1$, the exact solution is as follows:

$$\varphi(\xi,\mathfrak{t}) = \left(\sqrt{\mathfrak{c}}\,\mathrm{sec}\,h\left(\sqrt{\frac{\mathfrak{c}}{\mu(\mathfrak{c}+1)}}(\xi-(\mathfrak{c}+1)\mathfrak{t}-\xi_0)\right)\right), \tag{71}$$

and following the same steps mentioned earlier, we will obtain the following equation:

$$\rho_0(\xi) = \sqrt{\mathfrak{c}}\,\mathrm{sec}\,h\left(\sqrt{\mathfrak{c}(\mathfrak{c}+1)\mu}\,(\xi-\xi_0)\right),$$

$$\rho_1(\xi) = \frac{1}{\mathfrak{c}\mu+\mu}\left(6\mathfrak{c}^3\tanh^2\left(\sqrt{\frac{\mathfrak{c}}{\mathfrak{c}\mu+\mu}}(\xi-\xi_0)\right)\mathrm{sec}\,h^4\left(\sqrt{\frac{\mathfrak{c}}{\mathfrak{c}\mu+\mu}}(\xi-\xi_0)\right)\right),$$

$$\rho_2(\xi) = \frac{1}{(\mathfrak{c}+1)^4\mu^4}\left(62208\mathfrak{c}^{12}\sqrt{\frac{\mathfrak{c}}{\mathfrak{c}\mu+\mu}}\left(\cosh\left(2\sqrt{\frac{\mathfrak{c}}{\mathfrak{c}\mu+\mu}}(\xi-\xi_0)\right)-2\right)^2\tanh^5\left(\sqrt{\frac{\mathfrak{c}}{\mathfrak{c}\mu+\mu}}(\xi-\xi_0)\right)\mathrm{sec}\,h^{20}\left(\sqrt{\frac{\mathfrak{c}}{\mathfrak{c}\mu+\mu}}(\xi-\xi_0)\right)\right),$$
$$\vdots\,. \tag{72}$$

We can write the solution of (69) using the LRPS method as an infinite series.

$$\Phi(\xi,\mathfrak{S}) = \frac{\rho_0(\xi)}{\mathfrak{S}}+\frac{\rho_1(\xi)}{\mathfrak{S}^{\alpha+1}}+\frac{\rho_2(\xi)}{\mathfrak{S}^{2\alpha+1}}+\ldots \tag{73}$$

Applying the Laplace inverse to equation (73) can yield the kth approximate solution to our problem.

$$\varphi(\xi,\mathfrak{t}) = \rho_0(\xi)+\frac{\rho_1(\xi)\mathfrak{t}^{\alpha}}{\Gamma(\alpha+1)}+\frac{\rho_2(\xi)\mathfrak{t}^{2\alpha}}{\Gamma(2\alpha+1)}+\ldots \tag{74}$$

Table 4: Numerical results for FRLW equation (59) at $\mathfrak{c} = 0.03, \xi_0 = 0, \mu = 1$.

ţ	ξ	$\alpha = 0.6$	$\alpha = 0.75$	$\alpha = 1$
	−10	0.0373920	0.0366146	0.0354844
	−6	0.0584020	0.0575194	0.0565096
2	4	0.0872298	0.0878587	0.0889732
	6	0.0801849	0.0810171	0.0821916
	10	0.0579237	0.0587628	0.0596913
	−10	0.0356337	0.0337866	0.0304144
	−6	0.0545287	0.0524388	0.0492871
3	4	0.0872796	0.0887794	0.0920030
	6	0.0823111	0.0842877	0.0878101
	10	0.0618204	0.0638063	0.0667248
	−10	0.0343591	0.0303239	0.0214523
	−6	0.0467514	0.0421084	0.0338796
5	4	0.0836812	0.0869010	0.0954274
	6	0.0844980	0.0888261	0.0980846
	10	0.0699378	0.0743583	0.0819697

Table 5: Numerical results for FRLW equation (69) at $\mathfrak{c} = 0.03, \xi_0 = 0, \mu = 1$.

ţ	ξ	$\alpha = 0.6$	$\alpha = 0.75$	$\alpha = 1$
	−10	0.0608639	0.0608641	0.0608645
	−6	0.1102270	0.1102300	0.1102320
2	4	0.1394740	0.1394770	0.1394810
	6	0.1102270	0.1102300	0.1102320
	10	0.0608639	0.0608641	0.0608645
	−10	0.0608648	0.0608655	0.0608666
	−6	0.1102350	0.1102390	0.1102470
3	4	0.1394840	0.1394920	0.1395040
	6	0.1102350	0.1102390	0.1102470
	10	0.0608648	0.0608655	0.0608666
	−10	0.0608665	0.0608679	0.0608708
	−6	0.1102470	0.1102570	0.1102780
5	4	0.1395020	0.1395190	0.1395500
	6	0.1102470	0.1102570	0.1102780
	10	0.0608665	0.0608679	0.0608708

Our primary objective is to determine the numerical value of the third coefficient, ρ_2. It may be necessary to compute additional coefficients at a later time. Subsequently, we will compare the exact solution with the estimated solution derived from this series and closely scrutinize any discrepancies. This will enable us to evaluate the accuracy and dependability of the computed solution.

The outcomes obtained from applying the LRPS method to solve the FRLW equation (69) for various ţ and ξ values, in addition to different α values (specifically, $\alpha = 0.6, 0.75$ and 1), are presented in Table 5. We notice from the results of the tables a convergence of solutions at different values of α.

5. Graphical Illustrations

To illustrate the relationship between the various parameters of a solution, graphs are a powerful method. Hence, this section uses 2D and 3D graphs to show the solution $\varphi(\xi, ţ)$ with different values of α and ţ. The approximate solution of (25) is shown in Figures 1(a) and 1(b) for various values of α and ţ. We notice convergence of results despite the difference in values between α and ţ. Figures 1(c) and 1(d) show that for $\alpha = 1$, the approximate solution converges to the exact solution as α increases. Similarly, the solutions obtained through approximation for (35) are presented in Figures 2(a) and 2(b), depicting different values of α and ţ. Figures 2(c) and 2(d) demonstrate that as α increases, the accuracy of the approximate solution improves, approaching the exact solution for the case where α equals 1. Also, the approximate solutions of (45) are shown in Figures 3(a) and 3(b) for various values of α and ţ. We notice convergence of results despite the difference in values between α and ţ. Figures 3(c) and 3(d) show that for $\alpha = 1$, the approximate solution converges to the exact solution as α increases. Additionally, in order to provide a more accurate representation of the method's efficiency, we calculated the residual errors for the results of equations (25), (35), and (45) at different values of α. This is depicted in Figures 4(a)–4(c). Finally, Figures 5(a), 5(b), 6(a), and 6(b) show the approximate solution to the RLWE (52) and the MRLWE (69) for different values of α and ţ, illustrating a two-dimensional graph that displays the soliton wave solution. The graph plots $\varphi(\xi, ţ)$ against ξ and traces the wave trajectory for different α values. The results show that the outcomes obtained through fractional-order analysis converge to those obtained via integer-order analysis. Additionally, the second 2D graph presents the wave solutions for $\alpha = 1$ at different values of ţ, revealing that the soliton's amplitude remains constant while it moves to the right. Furthermore, in Figures 5(c), 5(d), 6(c), and 6(d), the shape of both the approximate and the exact solutions is represented, highlighting the convergence of the two solutions. Additionally, in order to provide a more accurate representation of the method's efficiency, we calculated the residual errors for the results of (59) and (69) at different values of α. This is depicted in Figures 7(a) and 7(b).

6. Discussion

In this section, we will review the results we have obtained in solving a set of nonlinear fractional partial differential equations using the LRPS method and compare these results with other methods used to solve the same applications. In Tables 6–8, we compare the solutions obtained using the LRPS method with those obtained using q-HATM [16] method for the first application, which represents the FKSE in its three cases. The results showed a convergence between the two methods for different values of α, as well as a convergence to the exact solution. Furthermore, in Table 9, which represents the absolute error results for RLWE equation (59), a comparison was made with the q-HATM method [28]. The results showed that the method used in this study provided much better solutions than the other method. Finally, a comparison was made between the absolute error results obtained using the proposed method and the HPSTM [27] method in Table 10, which represents the results of solving equation MRLWE (69). The results showed

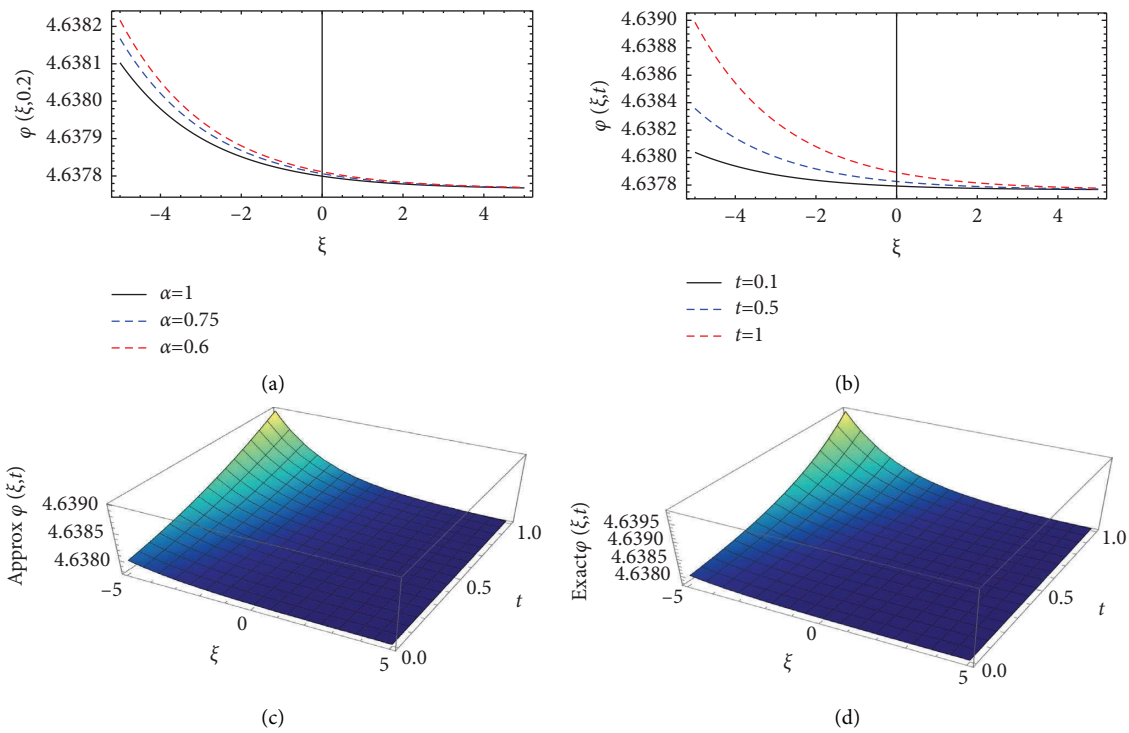

Figure 1: The solution of FKS (16) for $\mu = -1, \vartheta = 0, \delta = 1$. (a) Approx-solutions of equation (25) at different values of α. (b) Approx-solutions of equation (25) at different values of ţ. (c) LRPSM results at $\alpha = 1$. (d) Analytical results.

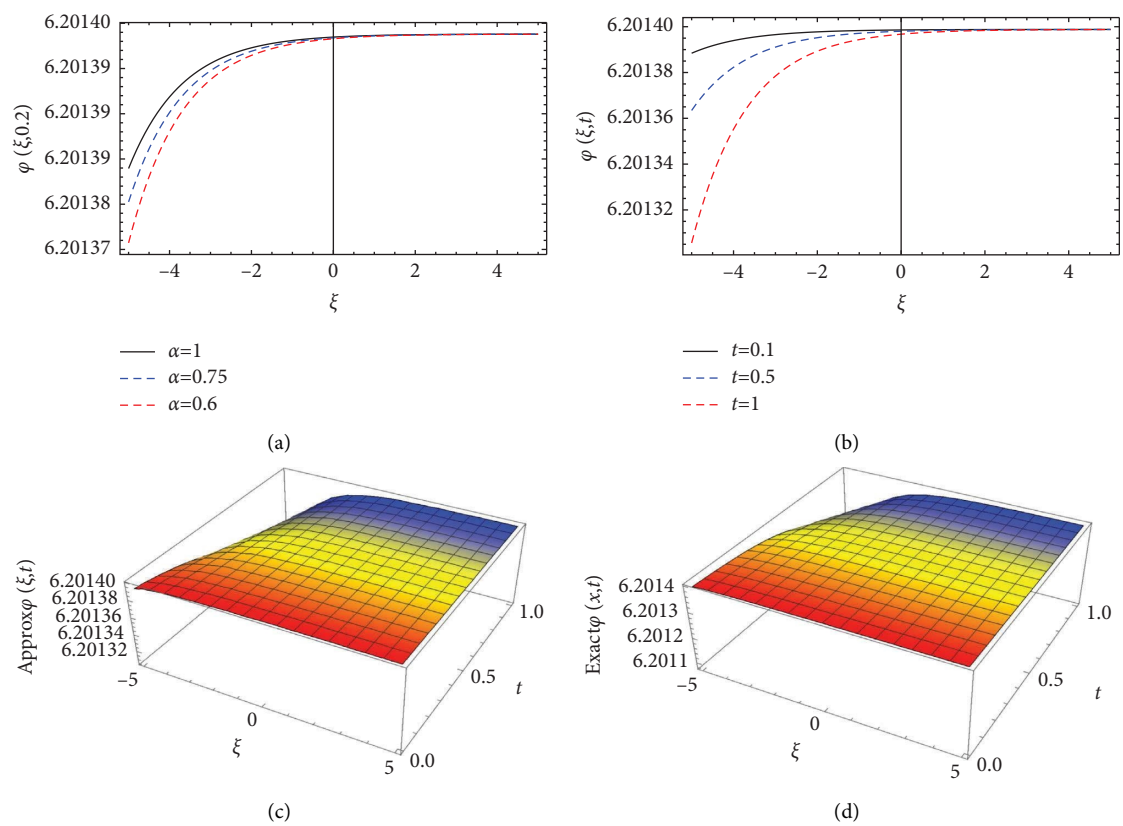

Figure 2: The solution of FKS (25) for $\mu = 1, \vartheta = 0, \delta = 1$. (a) Approx-solutions of (25) at different values of α. (b) Approx-solutions of (25) at different values of ţ. (c) LRPSM results at $\alpha = 1$. (d) Analytical results.

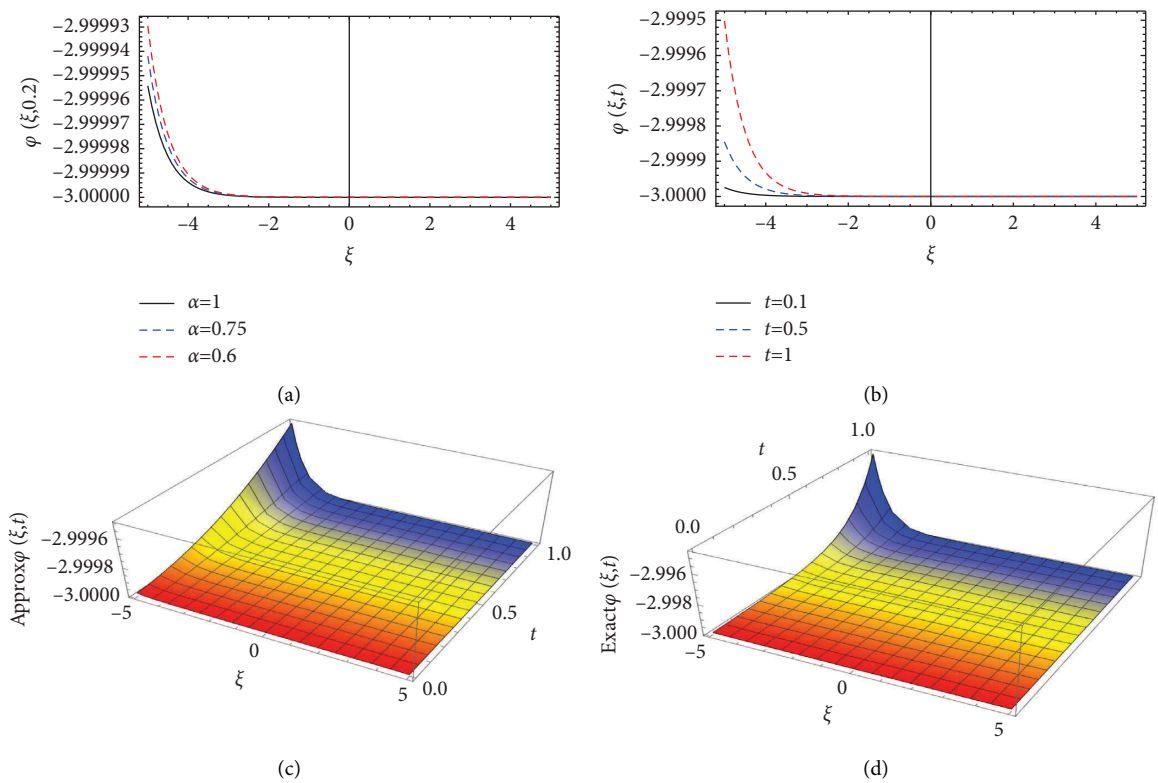

Figure 3: The solution of FKS (37) for $\mu = 1, \vartheta = 4, \delta = 1$ (a) Approx-solutions of (37) at different values of α. (b) Approx-solutions of (37) at different values of ţ. (c) LRPSM results at $\alpha = 1$. (d) Analytical results.

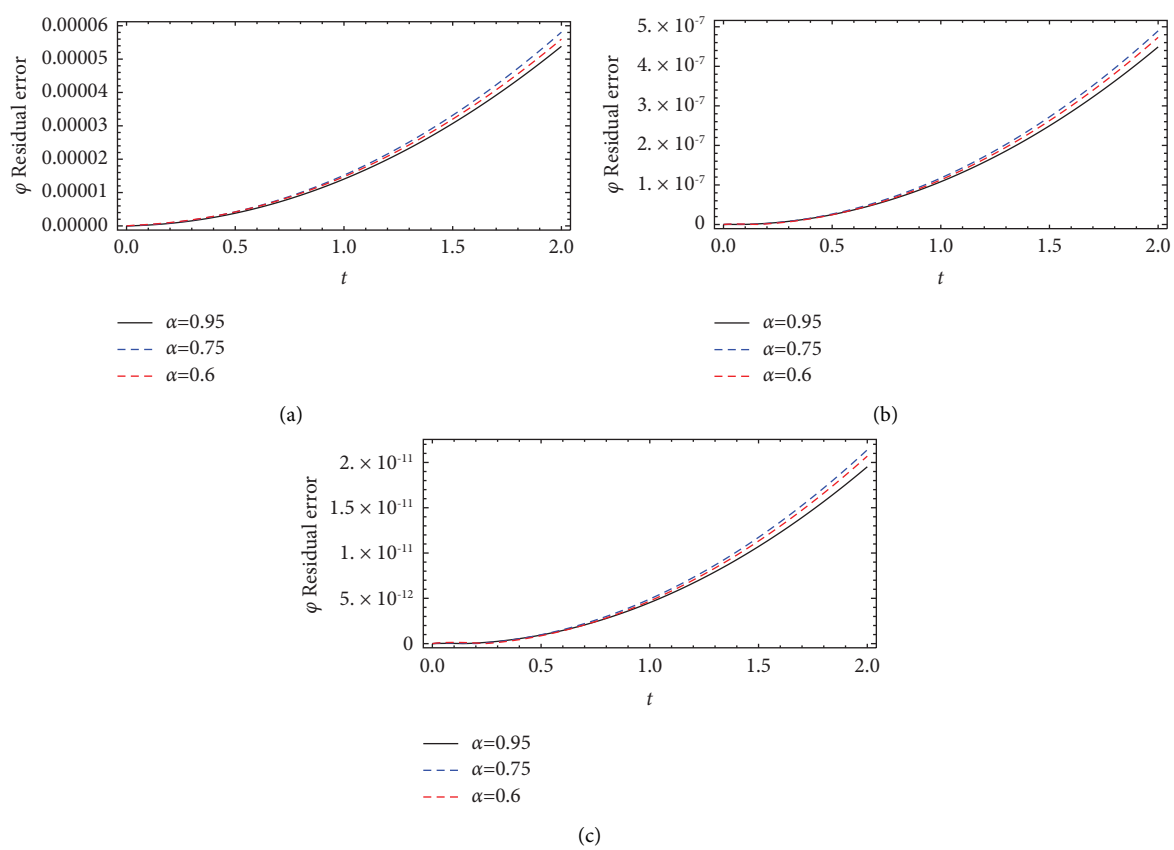

Figure 4: The residual error for application (1) at $\xi = 5, \alpha = 0.6, 0.75,$ and 0.95. (a) Residual error for equation (25) at $\beta = 5, \kappa = 1/2\sqrt{19}, \nu = -25$. (b) Residual error for equation (35) at $\beta = 5, \kappa = 0.5\sqrt{11/19}, \nu = -25$. (c) Residual error for equation (46) at $\beta = 5, \kappa = 0.5, \nu = -13$.

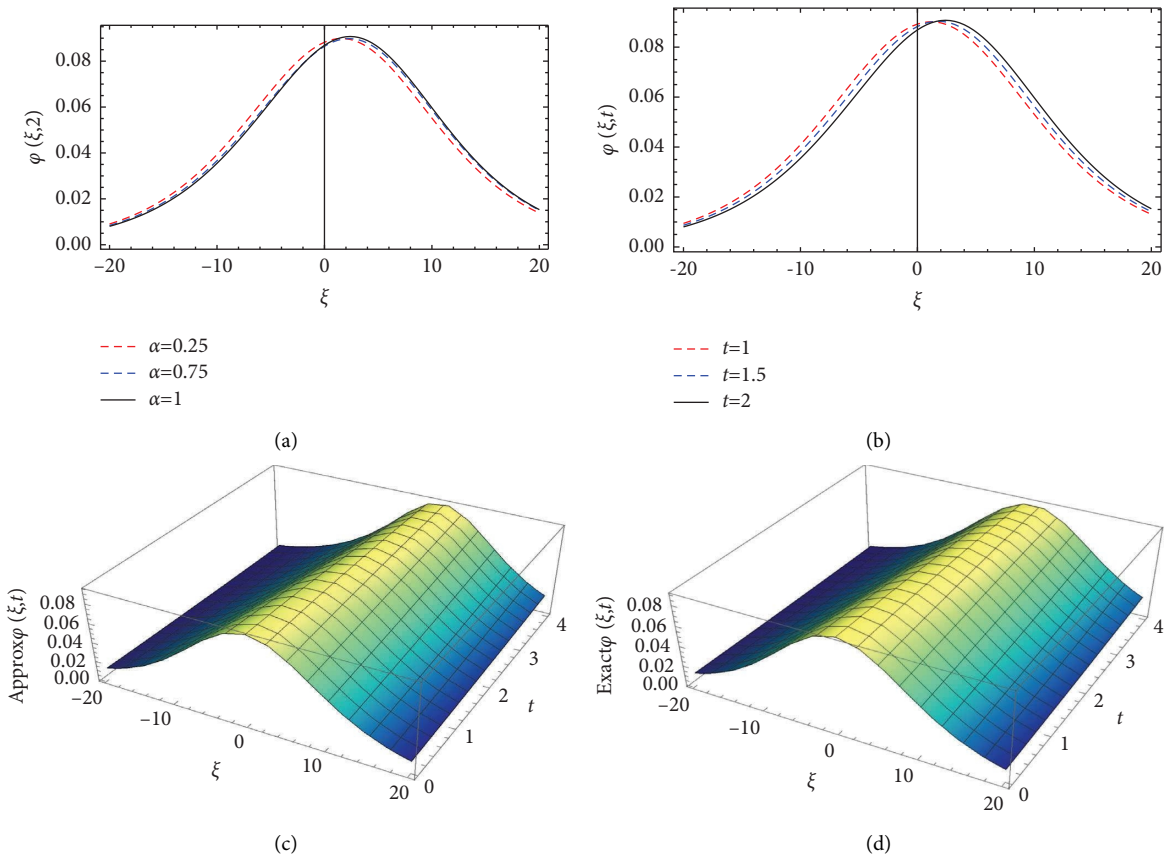

Figure 5: The solution of RLWE (59) for $\mathfrak{c} = 0.03, \mathrm{p} = 1, \mu = 1, \xi_0 = 0$. (a) Approx-solutions of equation (59) at different values of α. (b) Approx-solutions of equation (59) at different values of ţ. (c) LRPSM results at $\alpha = 1$. (d) Analytical results.

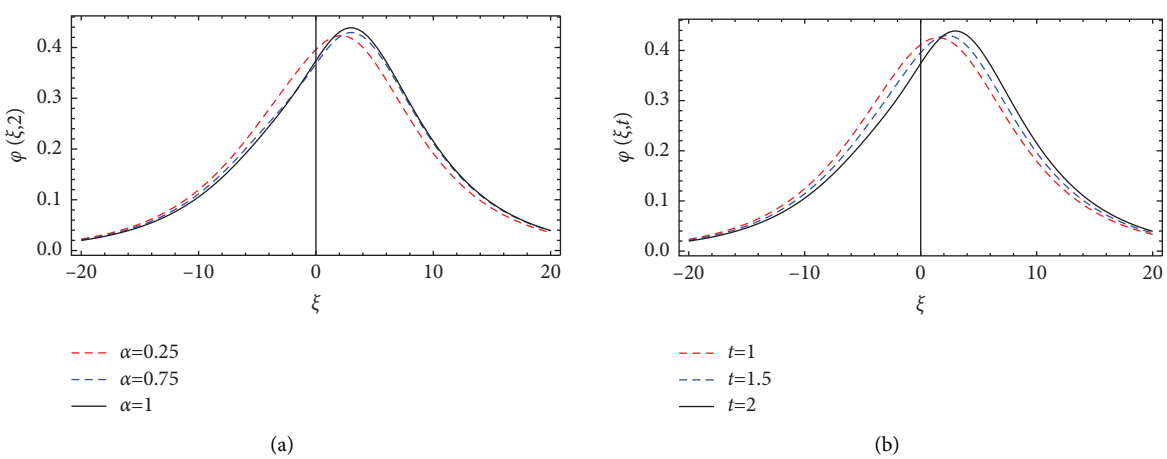

Figure 6: Continued.

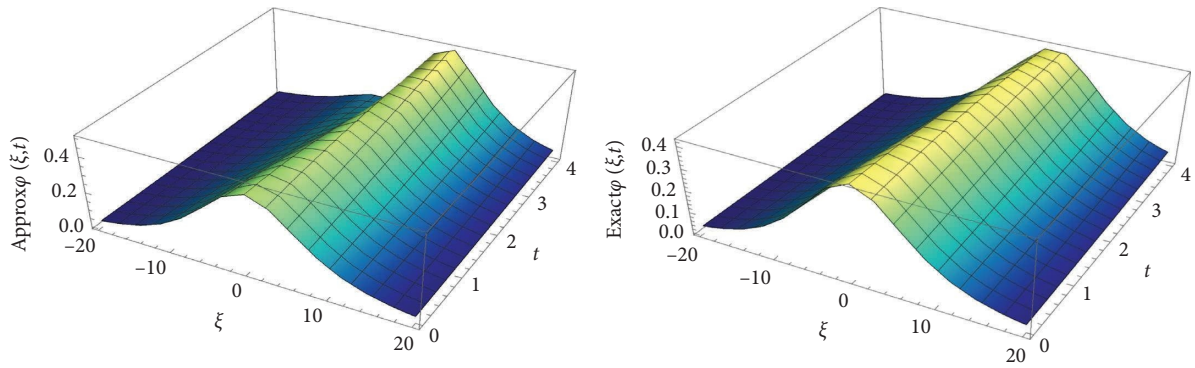

(c) (d)

Figure 6: The solution of the MRLWE (69) for $\mathfrak{c} = 0.3, \mathrm{p} = 2, \mu = 1, \xi_0 = 0$. (a) Approx-solutions of equation (69) at different values of α. (b) Approx-solutions of equation (69) at different values of ţ. (c) LRPSM results at $\alpha = 1$. (d) Analytical results.

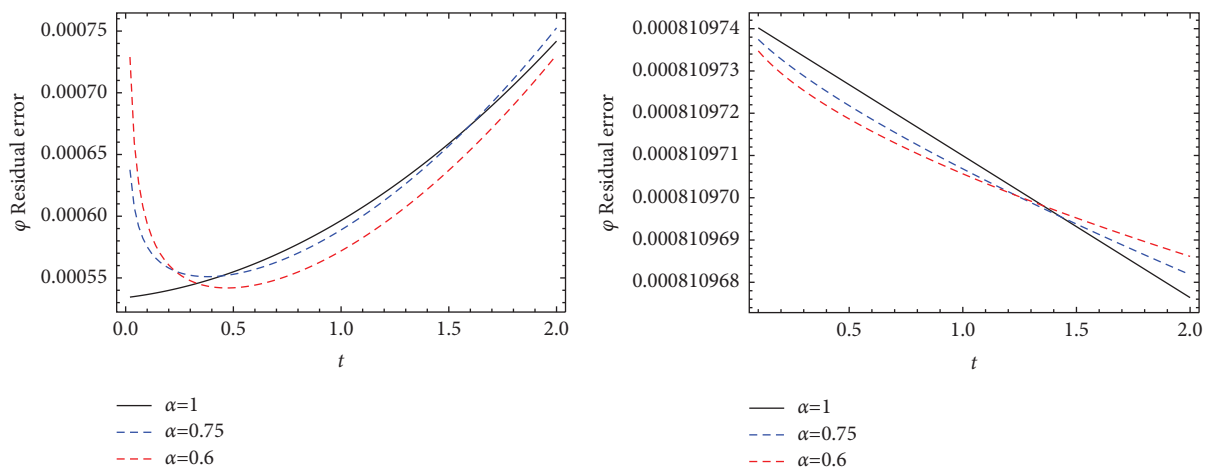

(a) (b)

Figure 7: The residual error for application (2) at $\xi = 5, \alpha = 0.6, 0.75$, and 1. (a) Residual error for FRLW equation (59) at $\mathfrak{c} = 0.03, \xi_0 = 0, \mu = 1$. (b) Residual error for FRLW equation (69) at $\mathfrak{c} = 0.03, \xi_0 = 0, \mu = 1$.

Table 6: Comparison between |Error| of q-HPTM [16] and LRPSM for equation (25) at $\beta = 5, \kappa = 1/2\sqrt{19}, \nu = -25, \alpha = 1$.

ξ	ţ	|Error| LRPSM	|Error| q-HATM [16]
2	0.2	1.102592×10^{-6}	1.785730×10^{-8}
	0.4	5.226914×10^{-6}	3.154480×10^{-7}
	0.8	3.049480×10^{-5}	6.268760×10^{-6}
	1	5.866110×10^{-5}	1.722960×10^{-5}
5	0.2	2.802116×10^{-7}	4.513880×10^{-9}
	0.4	1.329286×10^{-6}	8.086679×10^{-8}
	0.8	7.771472×10^{-6}	3.610840×10^{-7}
	1	1.497230×10^{-5}	4.434620×10^{-7}

Table 7: Comparison between |Error| of q-HPTM [16] and LRPSM for equation (35) at $\beta = 5, \kappa = 0.5\sqrt{11/19}, \nu = -25, \alpha = 1$.

ξ	ţ	|Error| LRPSM	|Error| q-HATM [16]
2	0.2	1.578621×10^{-9}	1.785730×10^{-8}
	0.4	2.499211×10^{-8}	3.154480×10^{-8}
	0.8	4.001540×10^{-7}	6.268760×10^{-6}
	1	1.095539×10^{-6}	1.722960×10^{-5}
5	0.2	1.610400×10^{-10}	4.573880×10^{-9}
	0.4	2.549514×10^{-9}	8.086670×10^{-8}
	0.6	1.238159×10^{-8}	4.552490×10^{-8}
	0.8	4.082080×10^{-8}	3.610840×10^{-7}
	1	1.117589×10^{-7}	4.434620×10^{-7}

that the proposed method outperformed the HPSTM [27] method in terms of accuracy. In general, this approach is highly effective and can be easily utilized for various nonlinear fractional partial differential equations along with their initial conditions. Furthermore, it offers a comprehensive framework that can be employed for different physical systems. Nevertheless, one drawback of this method is that it may not be suitable for all types of NFPDEs and the accuracy of the outcomes might rely on the specific system that is being modeled. Additionally, the method's constraints in terms of the fractional derivative order and time range should be taken into account. Despite these limitations, this proposed method is a significant contribution to the field of NFPDEs and opens up promising avenues for future research.

Table 8: Comparison between |Error| of q-HPTM [16] and LRPSM for equation (45)at $\beta = 3, \kappa = 0.5, \nu = -13, \alpha = 1$.

ξ	$\mathfrak{t}$	|Error| LRPSM	|Error| q-HATM [16]
2	0.2	9.006129×10^{-13}	5.078550×10^{-10}
	0.4	3.170086×10^{-11}	1.104840×10^{-8}
	0.6	2.380371×10^{-10}	3.883960×10^{-7}
	0.8	1.083714×10^{-9}	1.550600×10^{-6}
	1	4.114596×10^{-9}	6.873440×10^{-11}
5	0.2	3.552713×10^{-15}	2.738790×10^{-11}
	0.4	7.638334×10^{-14}	1.992290×10^{-10}
	0.6	5.915268×10^{-13}	9.629790×10^{-10}
	0.8	2.684075×10^{-12}	3.845100×10^{-9}
	1	1.019984×10^{-11}	3.751850×10^{-9}

Table 9: Comparison between |Error| of q-HATM [28] and LRPSM for equation (59) at $\mathfrak{c} = 0.03, \alpha = 1, p = 1$.

$\mathfrak{t}$	ξ	Exact solution	LRPS solution	|Error| LRPSM	|Error| q-HATM [28]
0.001	−25	0.00491095	0.00491097	1.6442×10^{-8}	4.2203×10^{-6}
	−20	0.01111010	0.01111010	1.3804×10^{-8}	9.5909×10^{-6}
	−15	0.02397620	0.02397620	6.2941×10^{-8}	2.0907×10^{-5}
	15	0.02398340	0.02398350	3.1500×10^{-7}	2.7845×10^{-5}
	25	0.00491263	0.00491262	1.6447×10^{-8}	5.8658×10^{-6}
0.005	−25	0.00490760	0.00490768	8.2159×10^{-8}	2.1051×10^{-5}
	−20	0.01110280	0.01110290	6.8985×10^{-8}	4.7840×10^{-5}
	−15	0.02396180	0.02396150	3.14505×10^{-7}	1.0429×10^{-4}
	15	0.02399790	0.02399820	3.15005×10^{-7}	1.3898×10^{-4}
	25	0.00491599	0.00491591	8.2293×10^{-8}	2.9279×10^{-5}

Table 10: Comparison between |Error| of HPSTM [27] and LRPSM for equation (69) at $\mathfrak{c} = 0.001, \alpha = 1, p = 2$.

$\mathfrak{t}$	ξ	Exact solution	LRPSM solution	|Error| LRPSM	|Error| HPSTM [27]
0.01	0	0.0316228	0.0316228	1.582721×10^{-9}	1.169755×10^{-9}
	0.1	0.0316226	0.0316226	3.003982×10^{-8}	1.161434×10^{-8}
	0.2	0.0316222	0.0316221	6.166087×10^{-8}	1.153139×10^{-8}
	0.3	0.0316214	0.0316214	9.327884×10^{-8}	1.143950×10^{-8}
	0.4	0.0316204	0.0316202	1.248921×10^{-7}	1.134949×10^{-8}
	0.5	0.0316190	0.0316188	1.564992×10^{-7}	1.126218×10^{-8}

7. Conclusion

In this paper, we have presented a new analytical method for solving nonlinear fractional partial differential equations, namely, the LRPS method. The LRPS method is based on the Laplace transform and the residual power series technique. We have applied the LRPS method to two nonlinear fractional partial differential equations: the fractional GRLWE and FKSE. We have shown that the LRPS method can provide accurate and efficient approximate solutions for these equations. We have also compared the LRPS method with some existing methods and found that the LRPS method has some advantages over them. The LRPS method is a simple and powerful mathematical tool that can be used to solve various nonlinear fractional partial differential equations arising in different fields of science and engineering.

Data Availability

Data sharing is not applicable to this article as no data sets were generated or analyzed during the current study.

Disclosure

The authors confirm that all the results they obtained are new.

Conflicts of Interest

The authors declare that they have no conflicts of interest.

Authors' Contributions

The first and second authors contributed to the planning and design of the study. The third author conducted data collection and analysis. The fourth and fifth authors made figure preparation, manuscript preparation, and editing. All authors reviewed the final version of the paper and agreed to publish.

References

[1] S. G. Samko, A. A. Kilbas, and O. L. Marichev, *Fractional Integrals and Derivatives: Theory and Applications*, Gordon & Breach, New York, NY, USA, 1993.

[2] I. Podlubny, *Fractional Differential Equations*, Academic Press, San Diego, CA, USA, 1999.

[3] X. J. Yang, H. M. Srivastava, and T. Machado, "A new fractional derivative without singular kernel: application to the modelling of the steady heat flow," *Thermal Science*, vol. 20, no. 2, pp. 753–756, 2016.

[4] H. Khan, U. Farooq, R. Shah, D. Baleanu, P. Kumam, and M. Arif, "Analytical solutions of (2+time fractional order) dimensional physical models, using modified decomposition method," *Applied Sciences*, vol. 10, no. 1, p. 122, 2019.

[5] N. H. Aljahdaly, A. Akgul, I. Mahariq, and J. Kafle, "A comparative analysis of the fractional-order coupled Korteweg-De Vries equations with the Mittag-Leffler law," *Journal of Mathematics*, vol. 2022, Article ID 8876149, 30 pages, 2022.

[6] Y. Keskin and G. Oturanc, "Reduced differential transform method for partial differential equations," *International Journal of Nonlinear Sciences and Numerical Stimulation*, vol. 10, no. 6, pp. 741–750, 2009.

[7] H. Khan, A. Khan, M. Al-Qurashi, R. Shah, and D. Baleanu, "Modified modelling for heat like equations within Caputo operator," *Energies*, vol. 13, no. 8, p. 2002, 2020.

[8] H. M. Srivastava, R. Shah, H. Khan, and M. Arif, "Some analytical and numerical investigation of a family of fractional-order Helmholtz equations in two space dimensions," *Mathematical Methods in the Applied Sciences*, vol. 43, no. 1, pp. 199–212, 2020.

[9] C. Phang, A. Kanwal, and J. R. Loh, "New collocation scheme for solving fractional partial differential equations," *Hacettepe Journal of Mathematics and Statistics*, vol. 49, no. 3, pp. 1107–1125, 2020.

[10] F. S. Md Nasrudin, C. Phang, and A. Kanwal, "Fractal-fractional advection-diffusion-reaction equations by Ritz approximation approach," *Open Physics*, vol. 21, no. 1, p. 2023, 2023.

[11] A. Nazari-Golshan, "Fractional generalized Kuramoto-Sivashinsky equation:Formulation and solution," *The European Physical Journal- Plus*, vol. 134, no. 11, p. 565, 2019.

[12] M. Richard, W. Zhao, and S. Maitama, "New analytical modelling of fractional generalized Kuramoto-Sivashinky equation via Atangana-Baleanu operator and transform method," *Journal of Ocean Engineering and Science*, vol. 20, pp. 14–56, 2022.

[13] R. C. Mittal and S. Dahiya, "A quintic B-spline based differential quadrature method for numerical solution of kuramoto-sivashinsky equation," *International Journal of Nonlinear Sciences and Numerical Stimulation*, vol. 18, no. 2, pp. 103–114, 2017.

[14] R. Shah, H. Khan, D. Baleanu, P. Kumam, M. Arif, and J. Taibah, "A semi-analytical method to solve family of Kuramoto-Sivashinsky equations," *Journal of Taibah University for Science*, vol. 14, no. 1, pp. 402–411, 2020.

[15] M. Kurulay, A. Secer, and M. Akinlar, "A new approximate analytical solution of Kuramoto- sivashinsky equation using homotopy analysis method," *Applied Mathematics and Information Sciences*, vol. 7, no. 1, pp. 267–271, 2013.

[16] P. Veeresha and D. G. Prakasha, "Solution for fractional kuramoto-sivashinsky equation using novel computational technique," *International Journal of Computational and Applied Mathematics*, vol. 7, no. 2, p. 33, 2021.

[17] T. B. Benjamin, "Internal waves of permanent form in fluids of great depth," *Journal of Fluid Mechanics*, vol. 29, no. 3, pp. 559–592, 1967.

[18] R. I. Nuruddeen, K. S. Aboodh, and K. K. Ali, "Investigating the tangent dispersive solitary wave solutions to the Equal Width and Regularized Long Wave equations," *Journal of King Saud University Science*, vol. 32, no. 1, pp. 677–681, 2020.

[19] O. Nikan, M. M. Arbshahi, and H. Jafari, "Numerical simulation of the nonlinear fractional regularized long-wave model arising in ion acoustic plasma waves," *Discrete and Continuous Dynamical Systems*, 2018.

[20] R. Nawaz, S. Islam, I. A. Shah, M. Idrees, and H. Ullah, "Optimal homotopy asymptotic method to nonlinear damped generalized regularized long-wave equation," *Mathematical Problems in Engineering*, vol. 2013, 13 pages, 2013.

[21] T. Eriqat, A. El-Ajou, M. Oqielat, Z. Al-Zhour, and S. Momani, "A new attractive analytic approach for solutions of linear and nonlinear neutral fractional pantograph equations," *Chaos, Solitons and Fractals*, vol. 138, Article ID 109957, 2020.

[22] M. Alquran, M. Ali, M. Alsukhour, and I. Jaradat, "Promoted residual power series technique with Laplace transform to solve some time-fractional problems arising in physics," *Results in Physics*, vol. 19, Article ID 103667, 2020.

[23] M. Z. Sarikaya and H. Ogunmez, "On new inequalities via riemann-liouville fractional integration," *Abstract and Applied Analysis*, vol. 2012, Article ID 428983, 10 pages, 2012.

[24] J. Hanna and J. Rowland, *Fourier Series, Transforms, and Boundary Value Problems*, Wiley, New York, NY, USA, 1990.

[25] A. El-Ajoua, "Adapting the Laplace transform to create solitary solutions for the nonlinear time-fractional dispersive PDEs via a new approach," *The European Physical Journal Plus*, vol. 136, pp. 1–22, 2021.

[26] O. A. Arqub, A. El-Ajou, and S. Momani, "Constructing and predicting solitary pattern solutions for nonlinear time-fractional dispersive partial differential equations," *Journal of Computational Physics*, vol. 293, pp. 385–399, 2015.

[27] A. Goswami, J. Singh, D. Kumar, S. Gupta, and Sushila, "An efficient analytical technique for fractional partial differential equations occurring in ion acoustic waves in plasma," *Journal of Ocean Engineering and Science*, vol. 4, no. 2, pp. 85–99, 2019.

[28] D. Kumara, J. Singha, and D. Baleanub, "A new analysis for fractional model of regularized long-wave equation arising in ion acoustic plasma waves," *Mathematical Methods in the Applied Sciences*, vol. 40, pp. 1–10, 2017.